Improving energy efficiency in pear storage through dynamic controlled atmosphere (DCA)

Hoang Minh Phan[1], Bert E. Verlinden[2], Maarten L.A.T.M. Hertog[1], Pieter Verboven[1], and Bart M. Nicolai[1,2]

[1] KU Leuven, BIOSYST-MeBioS, Leuven, Belgium

[2] Flanders Centre of Postharvest Technology, Leuven, Belgium

Keywords: Energy Efficiency, Pear, Storage, Dynamic Controlled Atmosphere, Postharvest, Supply Chain

Highlights

- Dynamic controlled atmosphere (DCA) storage decreases respiration of pear fruit
- Respiration heat accounts for 10-30 % of the total heat load
- DCA storage reduces the total heat load of a storage room by 8-16 %
- DCA generally maintains quality better than standard controlled atmosphere storage

Abstract

The energy efficiency of 'Conference' pear storage was assessed for different storage strategies, including dynamic controlled atmosphere (DCA) at different temperatures and controlled atmosphere (CA) at varying temperatures and O_2 levels. Storage at -1 °C in 3 kPa O_2 and 0.7 kPa CO_2 was used as a benchmark. Direct respiration measurements during the storage period showed that DCA reduced respiratory heat by 30-40 % compared with the benchmark, even at slightly elevated temperatures. A simulation-based energy assessment revealed that DCA could reduce the total heat load in a storage room by 8-16 %. Fan operation was found to account for the largest share of the total heat load (up to 50 %), while the respiratory heat contributed around 10-30 %. Among all experimental strategies, DCA at -1 °C reduced the total heat load by ~8 %, and maintained good firmness and skin colour without inducing internal browning after long-term storage. This makes it the most optimal approach to balance fruit quality and energy savings.

1. Introduction

'Conference' pear accounts for 43 % of the European pear production (Lieberz, 2024). Fruit typically require long-term storage to meet market demand throughout the year. However, after being harvested, their quality deteriorates due to cellular oxidative reactions. To slow down these quality-degrading processes, fruit are typically stored in refrigerated environments with controlled atmospheric conditions (CA), which involves lowering the oxygen partial pressure (O_2) and increasing carbon dioxide partial pressure (CO_2). This retards softening and yellowing of the fruit skin and extends their shelf-life (Weber et al., 2017; Wendt et al., 2024a). However, prolonged low-temperature storage with a refrigeration system consumes energy, affecting production costs and emissions considerably (East et al., 2013; Ambaw et al., 2016). According to Boschiero et al. (2019), the long-term storage of pome fruit accounts for 15.7 % of the energy demand and 17.7 % of the greenhouse gas emissions associated with the life cycle of these fruit from production to consumption.

In CA storage of 'Conference' pear fruit, O_2 is typically maintained at around 3 kPa, a level considered above the anaerobic compensation point of the fruit (ACP). This O_2 limit prevents fermentation-induced defects, which can lead to the production of off-flavours (Prange, 2018). Furthermore, according to Franck et al. (2007), at a very low O_2 level, the fruit cells have insufficient energy to maintain the integrity of their cellular membrane. Hence, the phenolic compounds in cellular compartments leak out and are oxidized to o-quinones, which results in internal browning of pear fruits in long-term storage. While the ACP may vary and is not known a priori, a dynamic controlled atmosphere system (DCA) adjusts the O_2 concentration to a lower level by employing a sensor to detect low O_2 stress when approaching the ACP. Different methods exist to detect this fruit stress, such as changes in the respiratory quotient (RQ, defined as the ratio of CO_2 production rate to O_2 consumption rate) or chlorophyll fluorescence, or volatiles, e.g., ethanol, associated with fermentation (Prange, 2018). As the O_2 level decreases below 3 kPa with DCA, fruit quality has been found to be better maintained (Bessemans et al., 2016; Büchele et al., 2023b; Wendt et al., 2024a).

Since CA storage reduces fruit respiration and the corresponding heat production, several strategies have been studied to reduce energy consumption in long-term storage while maintaining fruit quality. Nahor et al. (2005) used a discrete-continuous model for CA

storage of ‘Conference’ pear and found that step-wise loading saved more energy than batch-wise loading but reduced firmness. Gruyters et al. (2018) modelled adaptive on-off cooling strategies of ‘Jonagold’ apple in CA storage. They demonstrated that using a larger temperature differential (e.g., 0.7 °C) around the setpoint of 0.95 °C during long-term apple storage significantly increased energy consumption, despite no adverse effect on apple firmness. East et al. (2013) reported that a slight increase in the temperature setpoint of CA storage had little impact on apple quality, and avoiding refrigeration during peak electricity cost periods could cut the cost by approximately 40 % while causing only a 0.5 °C average fruit temperature fluctuation. However, these simulation-based strategies assumed that respiration remains static, depending solely on temperature and/or gas composition, for their energy estimation, which may oversimplify the actual physiology, as respiration evolves dynamically over time due to ripening (Johnston et al., 2002).

More recent research has increasingly focused on DCA storage as a promising approach to develop storage strategies that further reduce energy consumption while preserving high fruit quality. According to Kittemann et al., (2015), apple storage under DCA (0.7 kPa O_2, 1.5 kPa CO_2) used 20 % less energy than CA (1 kPa O_2, 2.5 kPa CO_2) at the same temperature. Verlinden et al. (2023) compared the energy saving for blueberry storage at 1 °C between DCA (0.5 kPa O_2) and CA (5 kPa O_2), resulting in a total energy savings of up to 10 %.

This study aims to quantify the effects of O_2 level and storage temperature on the respiration rate of ‘Conference’ pears throughout storage by directly measuring respiration rate in sealed storage containers. The results on dynamic respiration rates were used to assess the potential energy savings of DCA compared to CA storage, under both standard and elevated temperature conditions, using a simulation-based approach. Additionally, pear quality in shelf-life was measured in terms of firmness, skin colour, and internal browning, to enable a comprehensive comparison between DCA and CA for both energy efficiency and fruit quality. The study was conducted at both laboratory and industrial scales.

2. Materials and Methods

2.1. Laboratory experiment of pear storage

Experiments were carried out in two storage seasons: 2023-2024 and 2024-2025. All 'Conference' pears were harvested from the same orchard (Bierbeek, Belgium, at 50.818° N, 4.776° E), for each season at commercial maturity determined by the Flanders Centre of Postharvest Technology (VCBT). Once harvested, pear fruit were transported to and randomized at VCBT, and then cold-conditioned at -1 °C in regular air for three weeks according to commercial protocols. Afterwards, pear fruit were divided into batches and stored in air-tight polypropene containers (approximately 300 L). These containers were placed in cold rooms with different temperatures at VCBT. Within these containers, different CA and DCA treatments were applied.

Figure 1 displays the experimental design in both seasons. In the 2023-2024 season, fruit were harvested on September 5, 2023. After cold-conditioning period, two storage conditions were used: (-1 °C, 3 kPa O_2) and (-1 °C, DCA). In the 2024-2025 season, fruit were harvested on September 2, 2024. After cold-conditioning, seven storage conditions were implemented: (-1 °C, 1 kPa O_2), (-1 °C, 3 kPa O_2), (-1 °C, 5 kPa O_2), (+1 °C, 1 kPa O_2), (+1 °C, 5 kPa O_2), (0 °C, DCA), and (+1 °C, DCA).

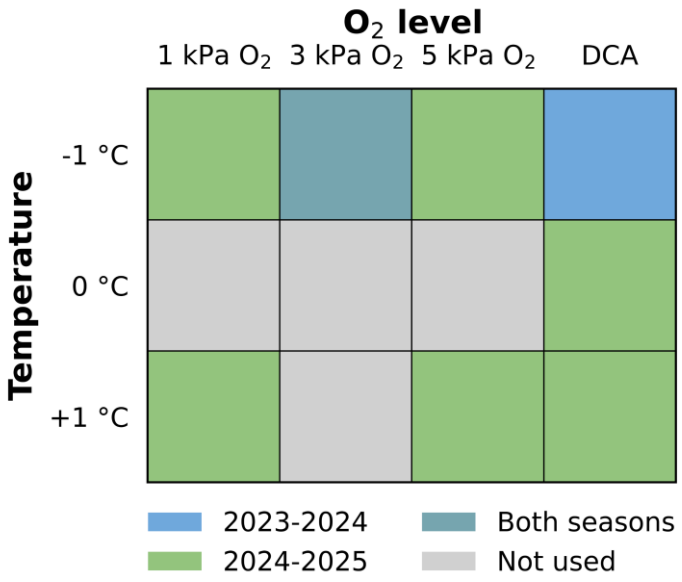

Figure 1. A combination of temperature and O_2 partial pressure for storage conditions in both seasons 2023-2024 and 2024-2025.

In all (D)CA treatments, the CO_2 level was kept at 0.7 kPa. During DCA, the O_2 partial pressure was dynamically controlled by the automated RQ measurement fitted to the container. The DCA controller was activated when the O_2 partial pressure reached 3 kPa, which was further adjusted downwards when RQ < 1.3 or upwards when RQ > 1.3, based on RQ determination every 11 h (Bessemans et al., 2016). The RQ determination was performed by measuring the CO_2 production rate (R_{CO_2}) and O_2 consumption rate (R_{O_2}) as described in section 2.2, and then calculated as follows.

$$\mathrm{RQ} = \frac{R_{CO_2}}{R_{O_2}} \quad \text{(Eq. 1)}$$

2.2. Respiration measurement during the storage period

The O_2 consumption and CO_2 production rates were measured for all CA and DCA containers (2024-2025) using a DCA controller (Bessemans et al., 2016), but during the 2023-2024 season, only the DCA container was monitored. Gas concentrations were measured over a 5 h period with the gas control system turned off. Based on the changes in O_2 and CO_2 levels, respiration rates were calculated and expressed per unit of fruit mass using the ideal gas law.

$$R_X = \frac{P_{total} V_{free}}{m_{fruit} R T_{air}} \cdot \left| \frac{\Delta X}{\Delta t} \right| \quad \text{(Eq. 2)}$$

where X = O_2 or CO_2; R_X is the corresponding respiration rate (mol $kg^{-1}s^{-1}$); P_{total} is the container pressure (Pa), V_{free} is the free-space volume (m^3) of the container; T_{air} is the absolute air temperature (K); m_{fruit} is the fruit mass (kg), ΔX is the change in the level of gas X (%); Δt is the period (s) without gas control; and R is the ideal gas constant (m^3 Pa K^{-1} mol^{-1}).

2.3. Industrial measurement of heat flux and fan power

In 2024-2025, an experiment was conducted in industrial rooms (Bierbeek, Belgium) to measure the heat load from the fan and the environment. Figure 2 presents the layout of the industrial rooms, each measuring 12 m (length) x 6.7 m (width) x 7.2 m (height). Rooms 1 and 2 were stored with 'Conference' pear at around -0.8 °C under (D)CA conditions. When two storage rooms were operated at DCA conditions, DCA treatment followed the principle described in sections 2.1 and 2.2, but applied to the whole room. For the heat flux measurement, five HFP01-heat-flux sensors (Hukseflux Thermal Sensors B.V., Netherlands) were placed around the rooms on the outside of the front and back walls and ceiling, and on the cold room

floor (Figure 2). The ambient temperature was measured by type-T thermocouples, located near the heat flux sensors of the front wall, back wall, and ceiling. Data were collected every 1 min using a DAQ970A data logger with a DAQM901A module (Keysight Technologies, Inc., USA). The heat flux (W m^{-2}) was assumed to be uniformly distributed on each surface. Finally, the average fan power in rooms 1 and 2 was logged at 15-min intervals, using power loggers (pSens2, Idetron Energy Management, Belgium).

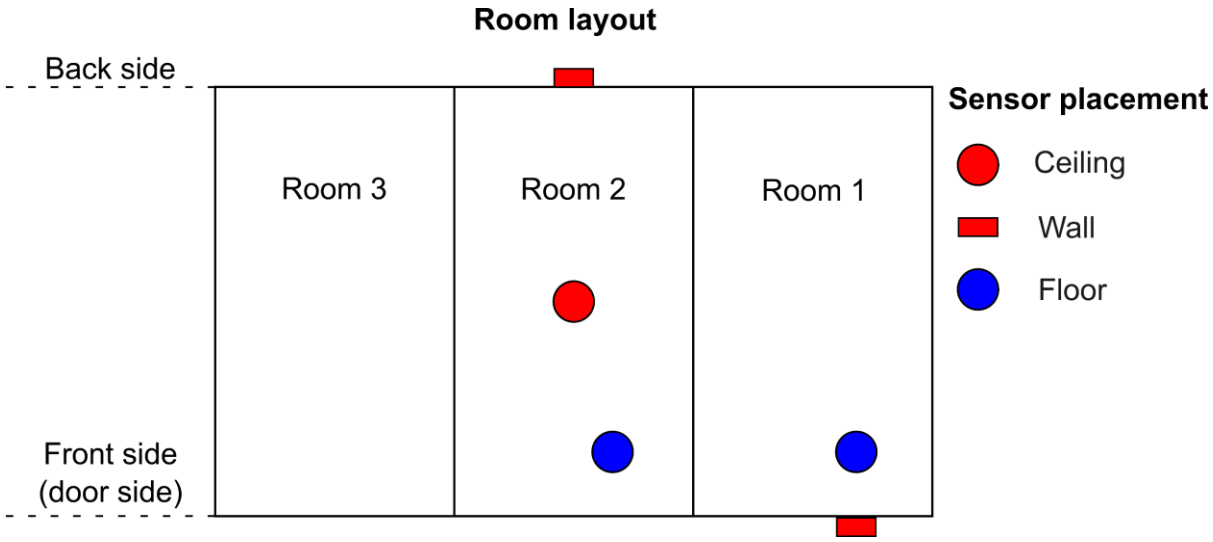

Figure 2. Layout of the storage rooms and placement of heat flux sensors in an industrial storage facility at Bierbeek, Belgium.

2.4. Simulation-based energy assessment in an industrial setting

Industrial storage facilities in Belgium usually rely on overfed liquid refrigeration systems to keep produce at low temperatures. However, under such systems, evaluating the energy consumption of individual cold storage rooms with different storage conditions is complex. Therefore, a simulation-based energy assessment was developed in our study. A simulation-based energy assessment procedure was implemented for different storage strategies at VCBT (section 2.1), incorporating all primary heat sources (fan heat, environmental heat, and respiratory heat) to reflect an industrial setting. A middle room, as representative of room 2, was selected for analysis. Assuming that the adjacent rooms had the same storage temperature, the environmental heat from side walls could be neglected. The room dimensions were defined in section 2.3.

The fan power was obtained from section 2.3 and kept constant to simulate fan heat load as explained further (section 3.3).

A heat flux model was developed using data in section 2.3 for simulating the environmental heat load. The heat flux q_s (W m^{-2}) through a room surface (s = walls, ceiling, or floor) was computed from:

$$q_s = U_s \left(T_\infty - T_{air} \right) \quad \text{(Eq. 3)}$$

where U_s is the corresponding overall heat transfer coefficient (W m^{-2} °C^{-1}); T_∞ and T_{air} are the ambient/soil and room-air temperatures (°C), respectively. In this paper, the U_s was assumed constant. To estimate its value, heat fluxes (q_s) and temperatures (T_∞ and T_{air}) in section 2.3 were split into a training dataset (60 %) and a test dataset (40 %). T_{air} of rooms 1 and 2 was obtained directly from the storage control system, while the soil temperature (T_∞) at 50 cm depth below the floor was retrieved from the Royal Meteorological Institute of Belgium.

The heat flux from the environment was then simulated using T_{air} from different storage conditions in both seasons (section 2.1), while T_∞ was taken only from the season 2024-2025. This choice avoids introducing variability caused by comparing data from the two different seasons (2023-2024 and 2024-2025), ensuring that differences in the simulation arise only from storage conditions, rather than external weather effects.

The respiratory heat was calculated based on the respiration rates in section 2.2.

$$q_{resp} = m_{fruit} \left[f_{ox} R_{O_2} + f_{fm} \max(R_{CO_2} - R_{O_2}, 0) \right] \quad \text{(Eq. 4)}$$

where q_{resp} is the heat of respiration rate (kW); m_{fruit} is the fruit mass (kg); R_{O_2} and R_{CO_2} are the measured O_2 consumption and CO_2 production rates (mol kg^{-1}s^{-1}), respectively; f_{ox} and f_{fm} are factors to convert oxidative respiration (468 kJ mol^{-1} O_2) and fermentation (36 kJ mol^{-1} CO_2) to heat, respectively, derived from Atkins and De Paula, (2011).

To mimic our industrial setting, the fruit mass was set to 147 tons to reflect the actual storage amount. It is important to note that for a conventional practice of (D)CA storage in Belgium, once (D)CA is applied, the storage rooms remain closed for long-term storage and are only opened at the end of the storage period to commercialize the entire batch of stored fruit. Therefore, there is no variation of the fruit mass in storage rooms during the long-term (D)CA storage. In exceptional cases, the room may be opened once for fruit quality assessment, but such an inspection does not significantly change the stored mass.

Finally, the simulation-based energy assessment of all experimental conditions was done by summing fan heat load, environmental heat load penetration through walls, and respiratory heat load as the total heat load. Since the respiratory heat was not modelled but measured, the simulation periods were strictly aligned with the measurement period. The total cumulative heat load (kWh) was calculated over November-January.

2.5. Physiological status of 'Conference' pear before storage

In each season, at the start of the storage experiment, but after the three-week conditioning period, 8-30 fruit were assessed for respiration and ethylene emission rate, firmness, and skin colour in regular air at 18 °C. Respiration and ethylene emission rates were measured following Ho et al. (2010) and Bulens et al. (2011), respectively. The skin colour was measured by a CM 2600d spectrophotometer (Konica Minolta Sensing Ltd., Singapore) on the shadow side of each pear at five points using the average hue angle. Next, fruit firmness was assessed using an SMS Texture Analyzer (Stable Micro Systems, UK) with a 300 N load cell. A cylindrical probe with a diameter of 8 mm was mounted on the load cell and moved toward the fruit at a constant speed of 8 mm s^{-1}. The maximum force (N) to penetrate the fruit to a depth of 8 mm was recorded at two equidistant points on the equator, one on the sun side and the other on the shadow side. Their average was used to represent the firmness of each fruit.

2.6. Shelf-life assessment for fruit quality

In both seasons, two-week shelf-life assessments were carried out at 18 °C in regular air after the cold-conditioning period (three weeks after harvest), and again after several months of storage, measuring colour, firmness, and internal browning of the pears. The 2023-2024 storage started from October 2023. Pear fruit stored at -1 °C in both 3 kPa O_2 and DCA were removed in February 2024 (after 4 months) for shelf-life assessment. During shelf-life, every 2 d, 15 pear fruit were destructively evaluated for skin colour, firmness, and internal browning. In the 2024-2025 season, the storage started from October 2024. In February 2025 (after 4 months), part of the fruit from CA storage at -1 °C in 3 kPa O_2 and DCA storage at 0 °C and +1 °C were removed for firmness and skin colour measurements. In March 2025 (after 5 months), part of the fruit from CA storage at -1 °C in 1 kPa, 3 kPa, and 5 kPa O_2, and CA storage at +1 °C in 1 kPa and 5 kPa O_2 were removed to measure firmness and skin colour. At the end of storage, in April 2025 (after 6 months), the remaining fruit were removed for internal browning inspection.

It should be noted that the DCA container at +1 °C was assessed twice (in February and April 2025). After February 2025, accurate RQ determination became difficult because the decrease

in fruit mass increased the free-space volume, making the changes in respiratory gas concentrations within an RQ-determination period too small to be detected reliably. Therefore, its O_2 level was fixed at the nearest O_2 level (0.5 kPa) in the DCA regime from February to April 2025, and considered a pseudo-DCA condition. Furthermore, every 2 d for each shelf-life assessment (2024-2025), firmness was measured destructively, so it remained independent with 10-20 new pear fruit, while the non-destructive measurements for colour were repeated on the same set of 8-18 pear fruit.

2.7. Quality measurement in shelf-life

For skin colour, pear images were captured with a digital camera in a controlled cabinet with standard LED lighting and fixed camera-to-subject distances (IPSS Engineering BV, Netherlands). The background skin colour (green-yellow) of each pear was segmented using a color analysis software (Wageningen University & Research, Netherlands). The pixel RGB values of the segmented area were then converted to CIE LCH and averaged for each fruit. The firmness measurement was described in section 2.5, while for internal browning, the fruit was cut in half along its length for inspection. The number of fruit with internal browning was counted and expressed as a percentage (Thewes et al., 2015).

2.8. Statistical analysis

For the pear sample at harvest (after the three-week cold condition), a two-sample comparison for the two seasons was conducted in JMP® 16 (JMP Statistical Discovery LLC, Cary, NC). If the normality assumption was valid, the t-test or Welch's test was used, depending on the homoscedasticity. Otherwise, the Mann-Whitney test was used.

For quality assessment in shelf-life, the effect of different storage conditions was compared at each measurement day. Depending on the data type, different procedures were used. For cross-sectional data, such as firmness from both seasons and colour in 2023-2024. If normality was satisfied, either one-way ANOVA or Welch's ANOVA was used, depending on the homoscedasticity. Otherwise, the Kruskal-Wallis test was applied. Afterwards, post hoc analyses included Tukey HSD (after one-way ANOVA), Games-Howell (after Welch's ANOVA), and the Mann-Whitney test with a *p*-value correction (after the Kruskal-Wallis test). This procedure was implemented in Python (v3.11) using scipy, statsmodels, and pingouin packages (Seabold and Perktold, 2010; Vallat, 2018; Virtanen et al., 2020). For longitudinal data, such as colour in 2024-2025, a mixed model was used to analyse the repeated

measurement, and then post hoc analysis (Tukey HSD) was used after confirming normality and homoscedasticity using JMP® 16 (JMP Statistical Discovery LLC, Cary, NC).

All statistical tests were conducted at a significance level of 5 %.

Parameter estimation of the heat flux model was implemented in Python (v3.11) using statsmodels for linear regression (Seabold and Perktold, 2010).

3. Results

3.1. Pear status after conditioning

The pear status after conditioning is shown in Table 1. The result indicates that despite a high variability and very low magnitude of ethylene emission rates, the fruit status after conditioning was comparable in both seasons.

Table 1. Pear fruit properties after a three-week conditioning period, measured in regular air at 18 °C. The mean and standard error are reported in the table. (*) indicates a significant difference in the mean values between the two seasons (p-value < 0.05).

Season	**2023-2024**		**2024-2025**	
	Sample size	Value	Sample size	Value
Harvest date	-	05-09-2023	-	02-09-2024
Measurement date	-	28-09-2023	-	27-09-2024
O_2 consumption rate ($\mu mol\ m^{-3}s^{-1}$)	10	139.7 ± 3.6	8	139.4 ± 3.3
CO_2 production rate ($\mu mol\ m^{-3}s^{-1}$)	10	125.8 ± 3.4	8	122.1 ± 2.9
Ethylene emission rate ($nmol\ m^{-3}s^{-1}$) *	10	2.11 ± 0.42	8	0.44 ± 0.14
Firmness (N) *	30	61.14 ± 0.82	10	56.3 ± 1.2
Hue angle (°)	30	102.72 ± 0.28	8	102.42 ± 0.51

3.2. Respiration rates during laboratory storage

The respiration rate (O_2 consumption rate and CO_2 production rate) and RQ under the five CA conditions from season 2024-2025 are shown in Figure 3. Storage at -1 °C in 3 kPa O_2 was considered the benchmark for comparison with other storage conditions, because it is the standard storage condition for 'Conference' pear. The respiration rate during CA storage at -1 °C in 1 kPa O_2 was the lowest, while storage at +1 °C in 5 kPa O_2 caused the highest respiration rate among the five containers. The respiration rate during storage at -1 °C in 5 kPa O_2 was similar to that of the benchmark. Furthermore, RQ measurements indicated that fruit stored at +1 °C in 1 kPa O_2 underwent strong fermentation with an RQ around 2, while the other

conditions exhibited only slight fermentation (RQ below 1.3). Additionally, the respiration rates increased over time, with their slope significantly higher than zero.

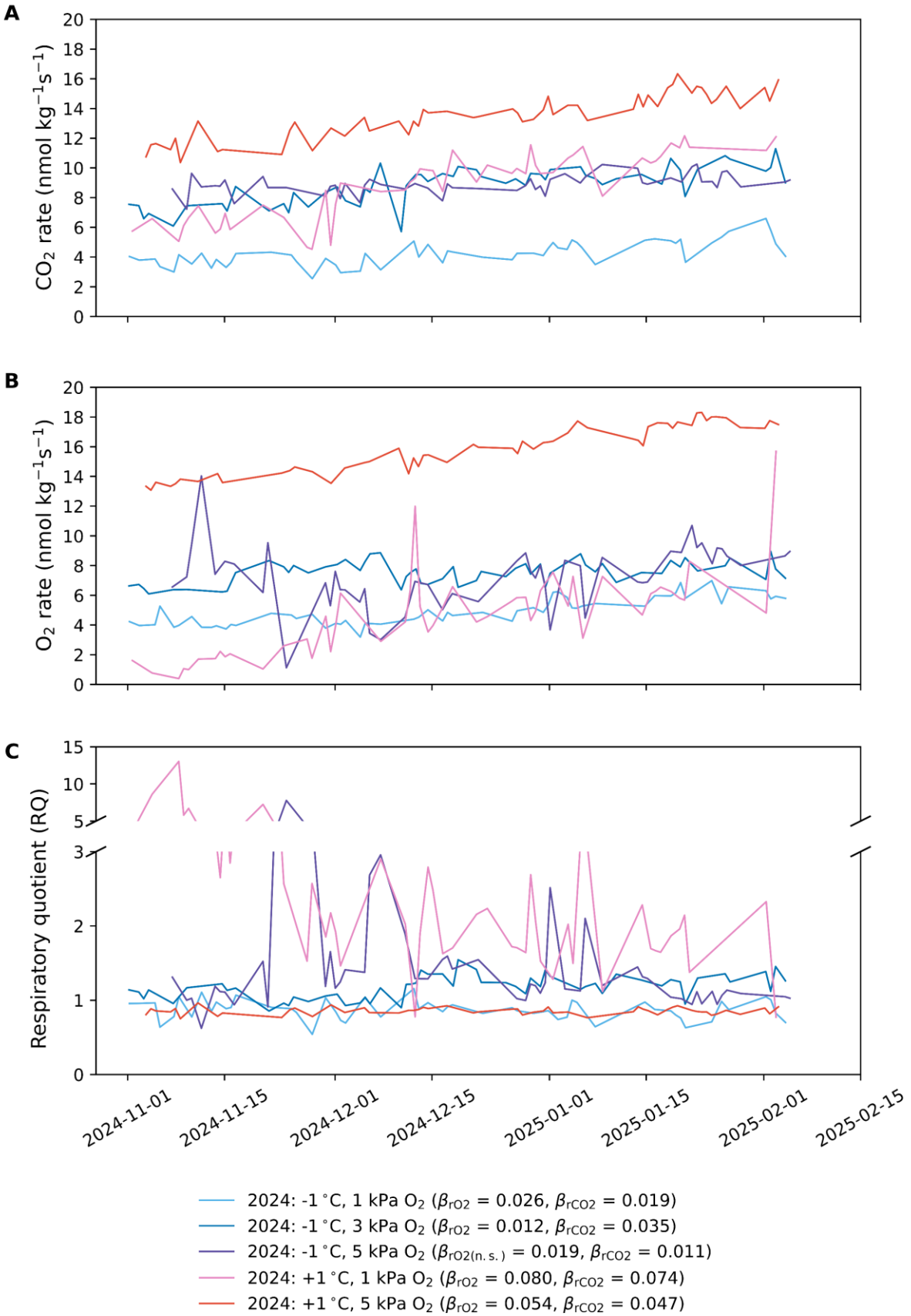
A
B
C
CO_2 rate (nmol $kg^{-1}s^{-1}$)
O_2 rate (nmol $kg^{-1}s^{-1}$)
Respiratory quotient (RQ)
2024-11-01
2024-11-15
2024-12-01
2024-12-15
2025-01-01
2025-01-15
2025-02-01
2025-02-15
2024: -1 °C, 1 kPa O_2 (β_{rO2} = 0.026, β_{rCO2} = 0.019)
2024: -1 °C, 3 kPa O_2 (β_{rO2} = 0.012, β_{rCO2} = 0.035)
2024: -1 °C, 5 kPa O_2 ($\beta_{rO2(n.s.)}$ = 0.019, β_{rCO2} = 0.011)
2024: +1 °C, 1 kPa O_2 (β_{rO2} = 0.080, β_{rCO2} = 0.074)
2024: +1 °C, 5 kPa O_2 (β_{rO2} = 0.054, β_{rCO2} = 0.047)

272

Figure 3. Measured respiration rate (A and B, nmol $kg^{-1}s^{-1}$) and RQ (C) in the 2024-2025 season in CA conditions. Data before November 1st, 2024, were excluded since fruit were still adapting to the CA environment. β (nmol $kg^{-1}s^{-1}d^{-1}$) represents the slope of the O_2 and CO_2 rates over time obtained from a simple linear regression between rates and storage day. A subscript (n.s.) indicates no significant difference of β from 0 (p-value > 0.05).

Figure 4 shows the respiration rates for DCA storage at -1 °C, 0 °C, and +1 °C, compared with the benchmark. Examining the O_2 profile and the respiration rate for DCA revealed that the respiration rate decreased or slowed down when the O_2 level decreased, especially below 1 kPa. Furthermore, the respiration rate during DCA storage at -1 °C and +1 °C was very similar and, in both cases, lower than that of the benchmark. The respiration rate during DCA storage at 0 °C was systematically higher than during the other DCA conditions, but comparable to that of the benchmark.

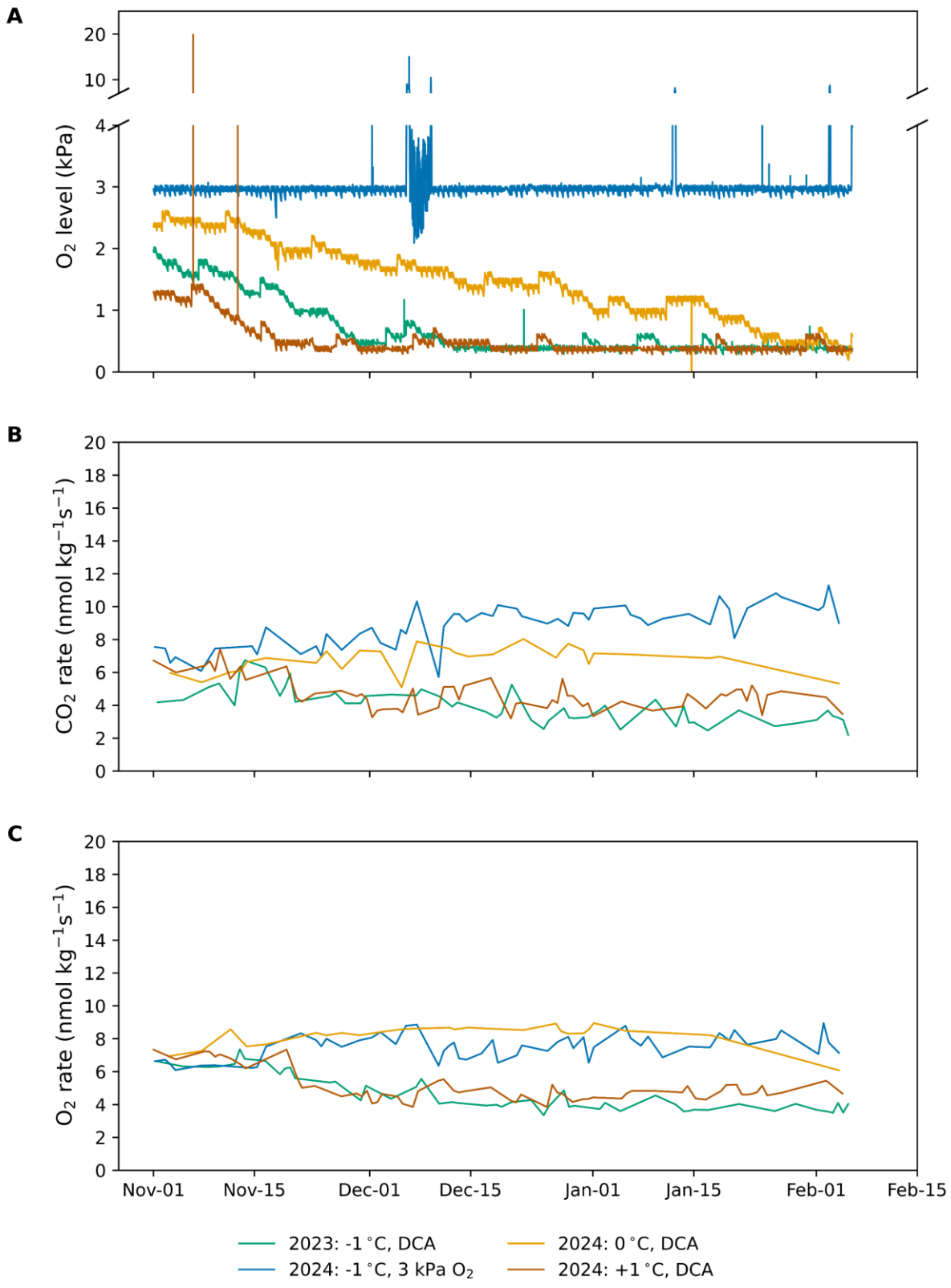

285

286 Figure 4. O_2 level (A, kPa) and measured respiration rates (B and C, nmol $kg^{-1}s^{-1}$) during the
287 2023-2024 and 2024-2025 seasons in DCA containers, compared to CA storage at -1 °C in 3
288 kPa O_2. Tick labels on the x-axis represent time scales in both seasons.

RQ measurements in DCA storage at -1 °C, 0 °C, and +1 °C, compared to the benchmark is shown in Figure 5. None of the DCA containers exhibited fermentation during the storage period.

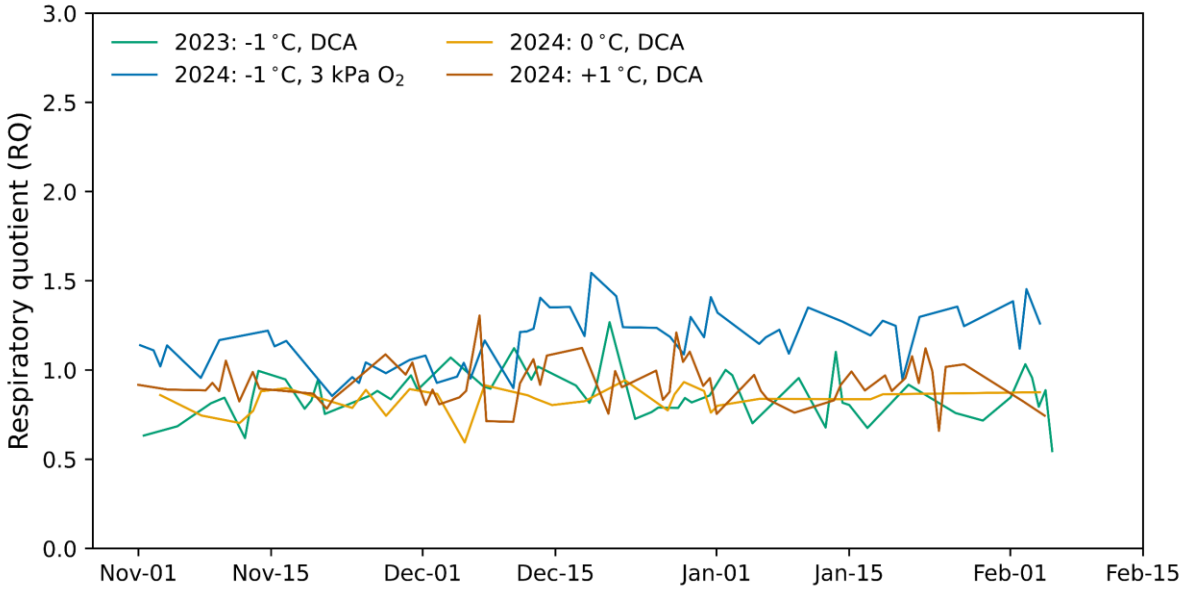

Figure 5. RQ measurement in DCA storage at -1 °C, 0 °C, and +1 °C, and CA storage at -1 °C in 3 kPa O_2.

3.3. Experimental measurement in industry

Figure 6 presents the storage condition of rooms 1 and 2. The temperature was close to -0.8 °C. The O_2 level was gradually reduced from above 3 kPa to around 1.5 kPa by DCA during storage.

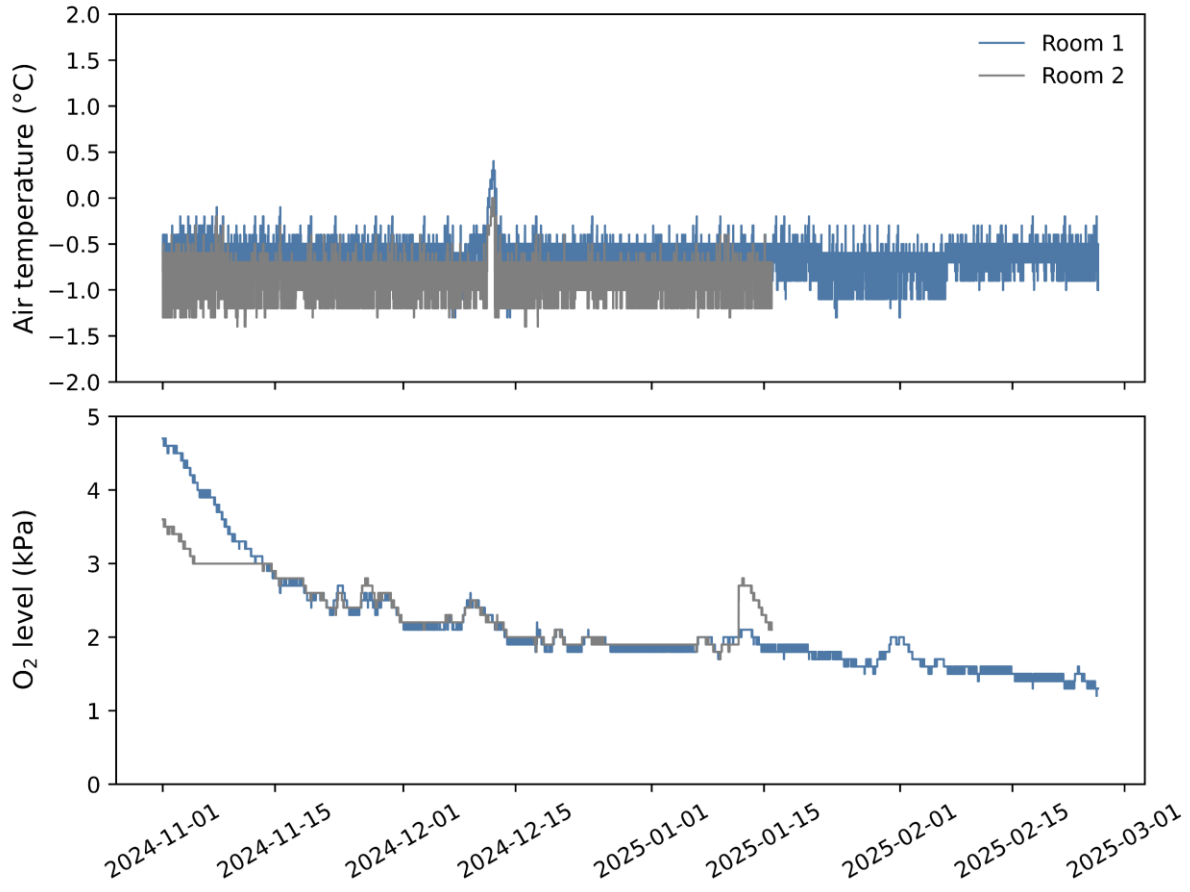

Figure 6. Storage conditions of Rooms 1 and 2 (Bierbeek, Belgium).

Figure 7 shows that the fan power of rooms 1 and 2 fluctuated around 1 kW. Due to limited data for different conditions, the fan power was assumed to be 1 kW to simulate its heat load.

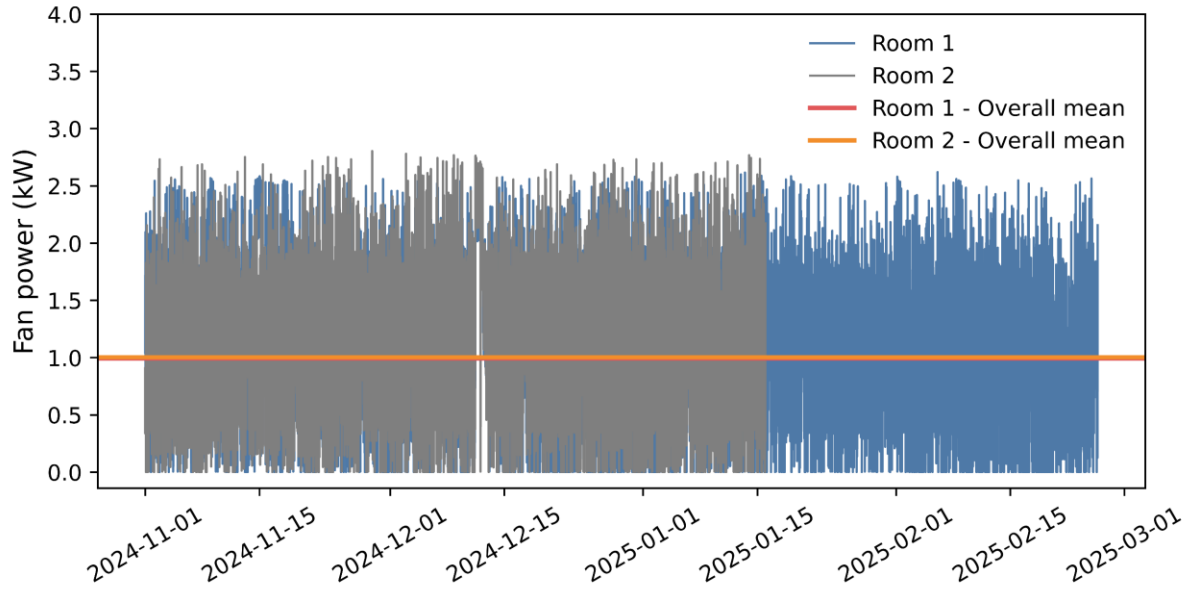

Figure 7. Measurement of fan power in rooms 1 and 2 in 2024-2025 (Bierbeek, Belgium). The overall mean fan power represents the average of the recorded fan power across the entire measurement period.

Figure 8 presents the calibration and validation results of the heat flux model for the front wall, selected as a representative example. The model fit had an R^2_{adj} of above 0.95.

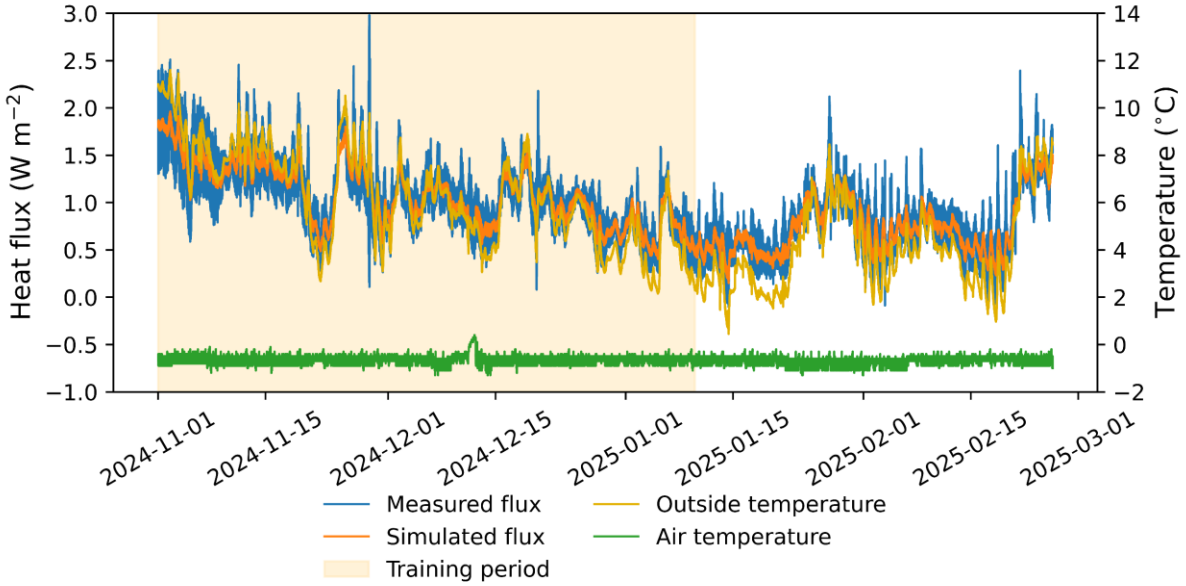

Figure 8. Heat flux at the front wall from the training and testing periods for the industrial facility (Bierbeek, Belgium).

3.4. Energy assessment for industrial CA and DCA rooms

Figure 9 shows the cumulative load of different heat sources after three months under all storage conditions. The benchmark (-1 °C, 3 kPa O_2) had a total heat load of 5446 kWh. DCA storage at -1 °C and CA storage at -1 °C and 1 kPa O_2 reduced the total heat load by around 8 %. Notably, DCA storage at +1 °C and CA storage at +1 °C and 1 kPa O_2 reduced the total heat load the most by around 16-18 %, by decreasing both the environmental and respiratory load. The total heat load during storage at +1 °C in 5 kPa O_2 was the highest, while during CA storage at -1 °C in 5 kPa O_2 and DCA storage at 0 °C, the heat load was similar to that of the benchmark. Moreover, across all conditions, the constant fan load contributed the most (40-50 %) to the total heat load, followed by the environmental heat (30-40 %), while the respiratory heat accounted for only 10-30 %.

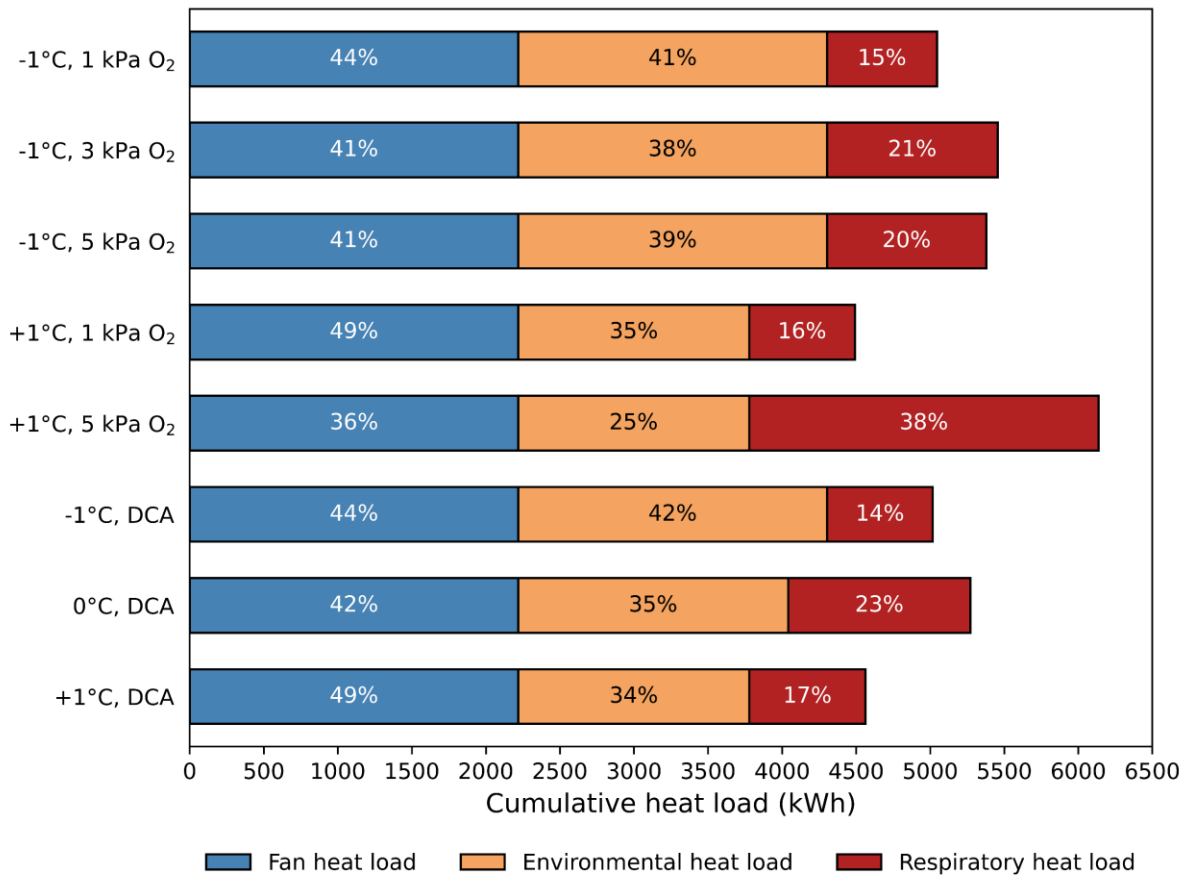

323

324 Figure 9. Total cumulative heat load from different storage strategies over three months
325 (November-January). Noted that (-1 °C, DCA) came from the season 2023-2024.

326 The monthly cumulative heat load (kWh) during storage at -1 °C in 3 kPa O_2 and DCA at -1
327 °C, 0 °C, and +1 °C is shown in Figure 10. Besides the stable fan load, the environmental heat
328 load fluctuated with the weather conditions, which reduced from November to January as
329 winter approached (Figure 8). The DCA conditions helped to reduce the respiratory heat load,
330 while this heat increased over time in the benchmark.

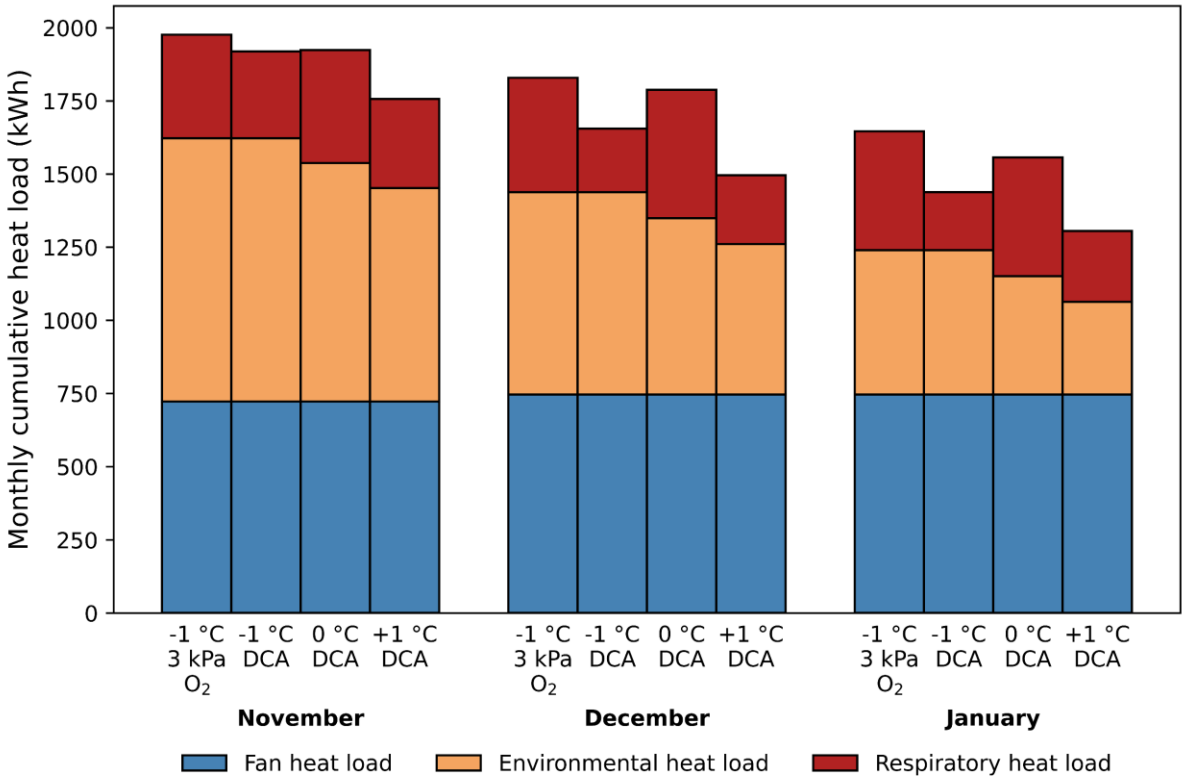

Figure 10. Monthly cumulative heat load from fan, environment, and respiration for (-1 °C, 3 kPa O_2), (-1 °C, DCA), (0 °C, DCA), and (+1 °C, DCA). Note that the (-1 °C, DCA) data were from season 2023-2024.

3.5. Quality evolution during shelf-life

The shelf-life quality of 'Conference' pear after five months of CA storage at -1 °C (1 kPa, 3 kPa, and 5 kPa O_2) and at +1 °C (1 kPa and 5 kPa O_2) is shown in Figure 11. Immediately after storage, the firmness from the high temperature and high O_2 condition (+1 °C, 5 kPa O_2) was the lowest and was reduced by 50 % compared to that at harvest. The three CA conditions at low temperature (-1 °C) maintained fruit firmness similar to that at harvest, while storage at high temperature and low O_2 partial pressure (+1 °C, 1 kPa O_2) resulted in a statistically significant but small reduction in firmness, compared with harvest. Next, the softening rate during shelf-life after storage was faster than at harvest. The pears from low temperature and low O_2 storage (-1 °C, 1 kPa O_2) maintained their firmness better than those in the other CA conditions until 4 d of shelf-life. By the end of shelf-life, the firmness was very low and the same for all CA conditions. Similar results were observed for pear skin colour. The pears from CA storage at +1 °C in 5 kPa O_2 had the lowest hue angle of about 105° after storage. In contrast, pear fruit stored at -1 °C in 1 kPa O_2 retained their greenness most effectively among

the CA conditions throughout shelf-life. The other CA conditions showed the same pattern of de-greening in which the hue angle dropped from approximately 110° to 98° over 10 d.

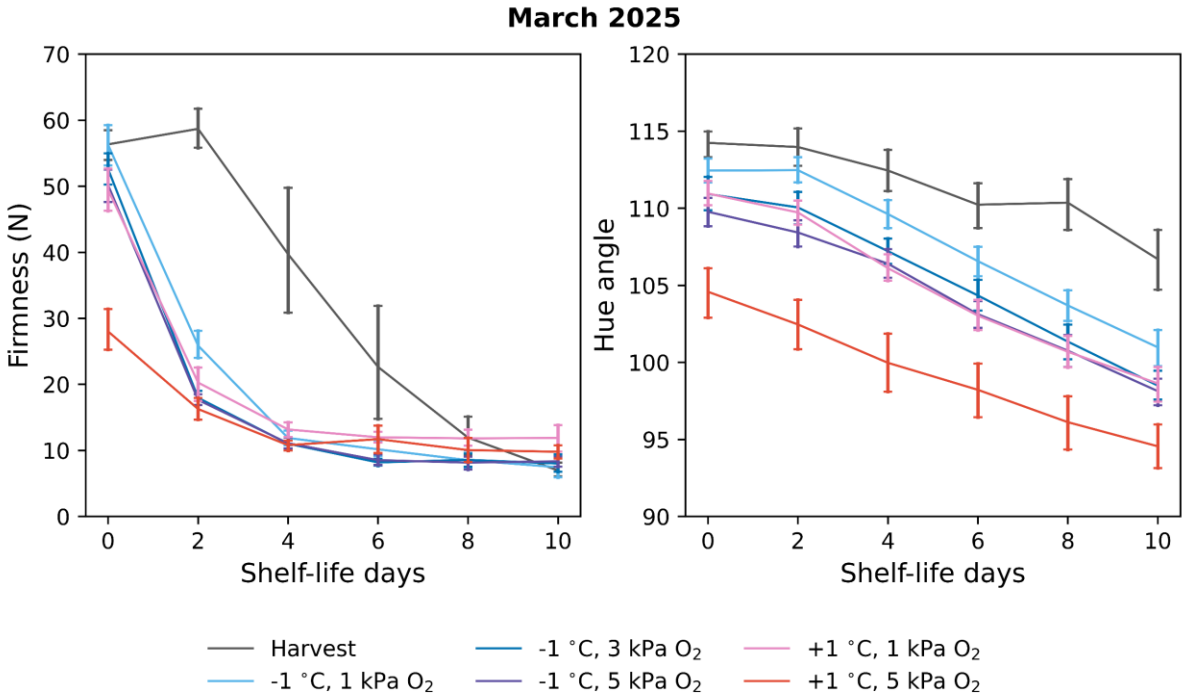

Figure 11. Firmness and hue angle of 'Conference' pear in shelf-life (March 2025) after 5 storage months at (-1 °C, 1 kPa O_2), (-1 °C, 3 kPa O_2), (-1 °C, 5 kPa O_2), (+1 °C, 1 kPa O_2), and (+1 °C, 5 kPa O_2), compared with that of pears at harvest (after 3-week cold conditioning). The error bar represents the 95 % confidence interval.

Next, the shelf-life quality of 'Conference' pear from DCA at different temperatures compared to the benchmark (-1 °C, 3 kPa O_2) is shown in Figure 12. The firmness immediately after storage was similar between the storage conditions and harvest. During shelf-life, the pears from DCA at 0 °C and +1 °C exhibited similar firmness patterns without a significant difference from the benchmark. In contrast, the pears stored under DCA at -1 °C had a delayed softening until 4 d, compared with those in the benchmark. The hue angle was not significantly different among different DCA conditions and the benchmark, although after storage, the pears were more yellow than those at harvest.

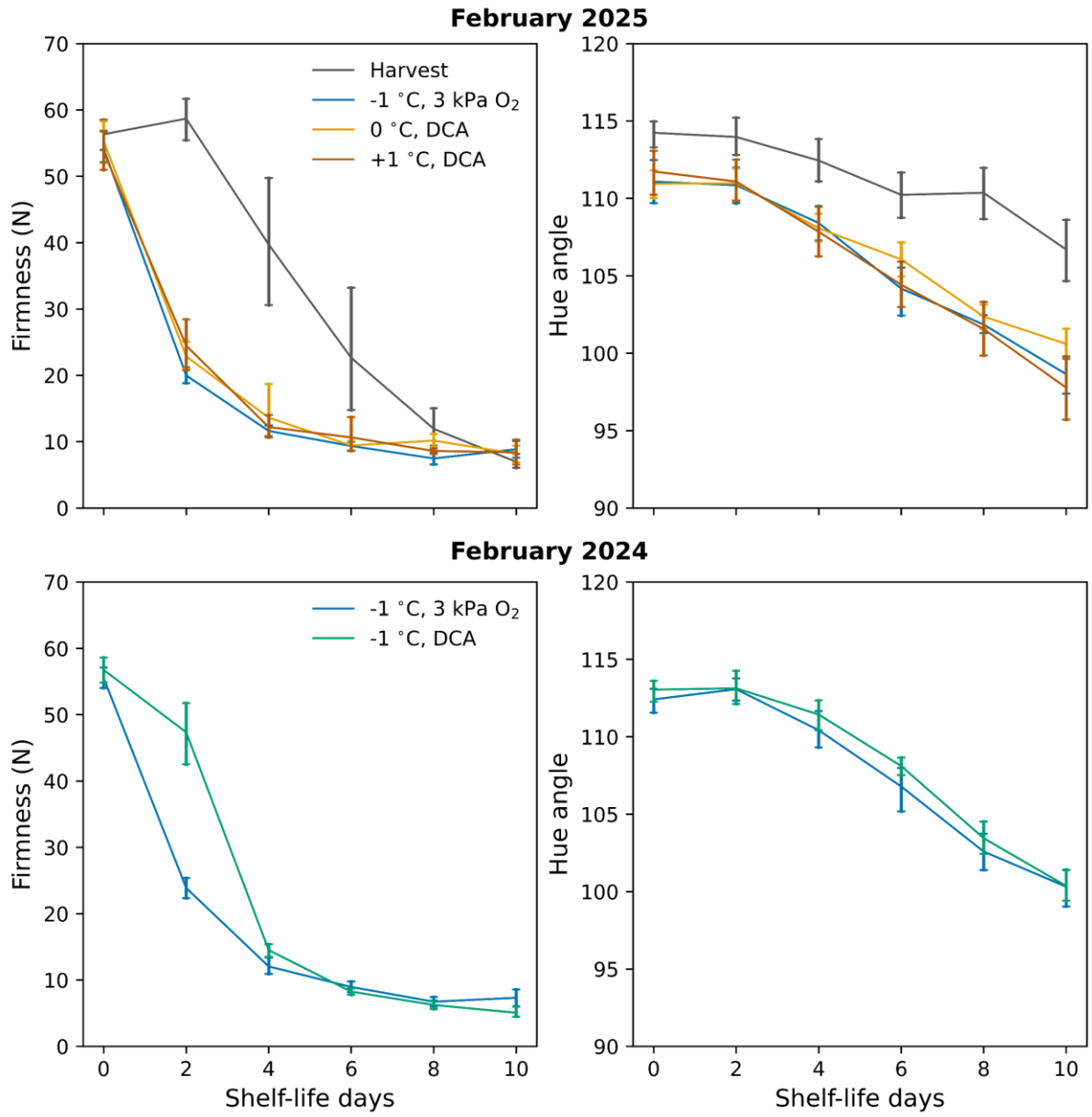

Figure 12. Firmness and hue angle of 'Conference' pear in shelf-life after 4 months storage at (-1 °C, 3 kPa O_2), (0 °C, DCA), and (+1 °C, DCA) in season 2024-2025, and (-1 °C, 3 kPa O_2) and (-1 °C, DCA) in season 2023-2024. The error bars represent 95 % confidence intervals.

Figure 13 presents the percentage of internal browning and core breakdown of 'Conference' pears in two seasons after storage. The pears stored at +1 °C exhibited a high browning incidence of at least 15 %, while those at -1 °C also had no browning incidence. Especially, pears under DCA at +1 °C had 15 % of browning incidence, but no browning was found in those under DCA at -1 °C. Data for DCA storage at 0 °C were unavailable since this ended in February 2025.

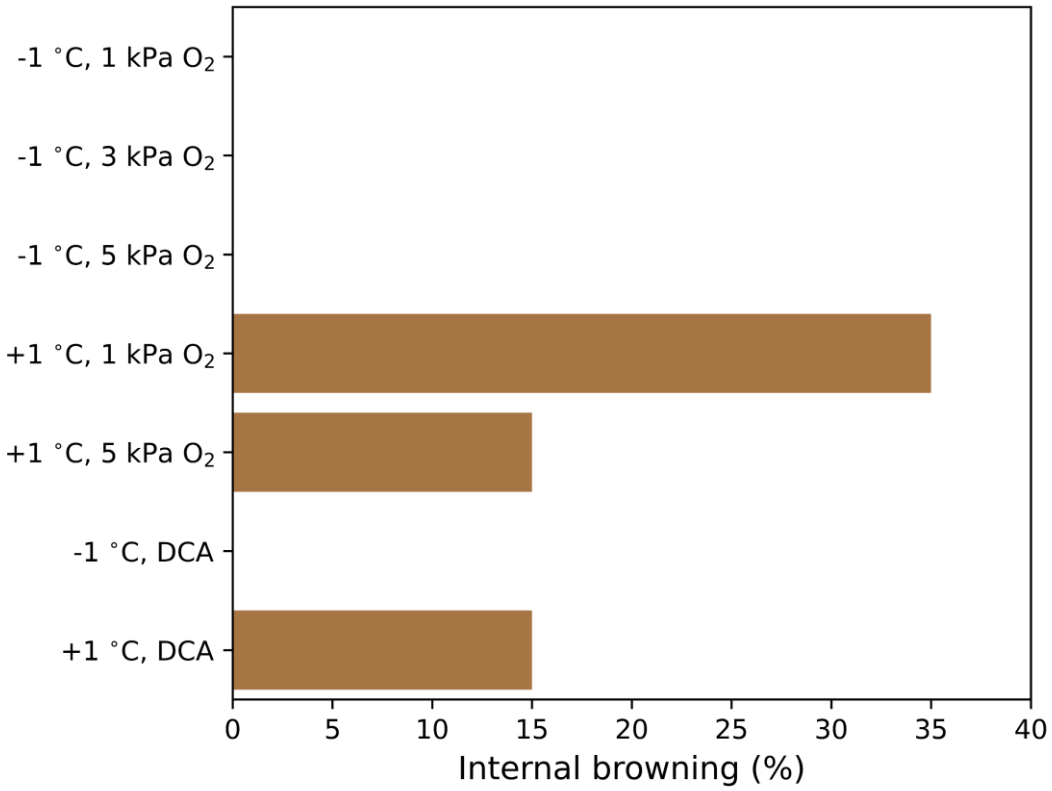

374

375 Figure 13. Internal browning (%) of 'Conference' pear in February 2024: (-1 °C, 3 kPa O_2) and
376 (-1 °C, DCA), and in April 2025: (-1 °C, 1-3-5 kPa O_2), (+1 °C, 1-5 kPa O_2), and (+1 °C, DCA),
377 measured one day after removal from storage.

378

4. Discussion

Respiration rate is usually expressed as the O_2 consumption rate and the CO_2 production rate. The O_2 consumption rate reflects oxidative respiration, while the CO_2 production rate includes both oxidative respiration and fermentation. Our measurements showed that oxidative respiration rate, i.e., O_2 consumption rate, had a positive relationship with the O_2 level and temperature in storage (Figure 3), similar to other studies (De Wild et al., 1999; Lammertyn et al., 2001; Ho et al., 2018). Furthermore, at the lower O_2 level and the higher temperature, the pears become more susceptible to fermentation during storage, as shown in CA storage at +1 °C in 1 kPa O_2 (Figure 3). In general, oxidative respiration and fermentation respond inversely to the O_2 level. As the O_2 level decreases to or below ACP, the oxidative respiration decreases while the fermentation increases (Boeckx et al., 2019). Next, the respiration rate dynamically evolved during the CA storage, and the change in respiration rate was even more complex during DCA storage. Johnston et al. (2002) observed a similar increasing trend of the respiration rate with time for apple cultivars at 0.5 °C in regular air. In contrast, Saquet and Streif, (2017) reported that the respiration rate of 'Conference' pear and 'Jonagold' apple in CA (0 °C, 1-3 kPa O_2) decreased during the first three months, then stabilized; furthermore, storing fruit below 1 kPa O_2 induced fermentation, partially contributing to respiratory heat. Therefore, estimating energy consumption in fruit storage under the assumption of constant respiratory heat production may inaccurately estimate the actual energy needed.

The respiration rate during DCA storage followed the trajectory of the O_2 partial pressure (Figure 4). The respiration rates of both DCA conditions (-1 °C and +1 °C) were very similar, and the O_2 partial pressure profile had a similar pattern. In contrast, the O_2 level during DCA storage at 0 °C remained consistently higher than during DCA at -1 °C and +1 °C, which leads to a higher respiration rate. The higher O_2 level observed in DCA storage at 0 °C resulted from fewer control actions of its DCA controller to lower the O_2 level because the measured RQ values did not satisfy the validity criteria enforced by the system as installed by the DCA control supplier (no data available). As a consequence, the O_2 level of DCA at 0 °C did not decrease as fast as expected. Furthermore, during DCA storage at 0.5 kPa O_2, the respiration rate not only decreased but also evolved very slowly or almost stayed constant, compared to other CA conditions at the same temperature. Also, no fermentation was induced in all DCA conditions, while CA storage at +1 °C in 1 kPa O_2 triggered fermentation. This aligns with the findings of Bessemans et al. (2016) who reported that DCA could reduce the O_2 level further without triggering fermentation.

DCA treatments generally resulted in a reduced total heat load compared to CA storage if their O_2 level was below 1 kPa O_2, which would reduce their respiratory heat by 30-40 %, compared to the benchmark (-1 °C, 3 kPa O_2) (Figure 4 and Figure 9). DCA storage at +1 °C reduced the total heat load more than DCA storage at -1 °C (16 % and 8 %, respectively) because DCA storage at +1 °C benefits from both reduced environmental heat and respiratory heat loads due to the high temperature and low O_2 levels (Figure 9). Next, for DCA storage at 0 °C, the heat load was not much different from the benchmark because of the high temperature and O_2 level that led to higher respiration. Kittemann et al. (2015) reported that for apple, 20 % of total energy use could be saved by DCA storage compared with CA storage in 1 kPa O_2 and 2.7 kPa CO_2 at 1 °C, which is somewhat higher than our experiments. A comparison between storage at -1 °C and +1 °C in 5 kPa O_2 showed that, although elevating the storage temperature helps in reducing the environmental heat load, the temperature increased the respiration heat considerably. On the other hand, although the CA storage at +1 °C in 1 kPa O_2 reduced the total heat load more than that at -1 °C in 1 kPa O_2, it induced fermentation. Furthermore, the increase of the respiration rate was even accelerated at a higher temperature in Figure 3. Ho et al. (2008) reported that temperature indeed has a strong impact on fruit respiration during storage. In addition, increasing the storage temperature setpoint also improves the refrigeration system performance. With the evaporating temperature increased by 1 °C, it typically improves about 3 % refrigeration system performance (Llopis and Martínez-Ángeles, 2026). However, as mentioned in section 2.4, the industrial storage systems in Belgium are usually equipped with overfed liquid refrigeration, which makes it challenging to assess the refrigeration-side performance when many storage rooms operate under varying conditions. Therefore, in this paper, we mainly focused on assessing energy at the storage room level.

The shelf-life quality assessment showed that firmness and colour of 'Conference' pear were affected by temperature and O_2 level during storage. The higher temperature facilitated the softening process, while the lower O_2 condition helped maintain the green skin color (Figure 11). This is in agreement with the results of Thewes et al. (2015) and Wendt et al. (2024b). Furthermore, Figure 12 revealed that during shelf-life, DCA storage generally maintained pear quality better than CA storage, which was also observed by Thewes et al., (2020) for apples. Our findings confirmed that DCA at elevated temperatures (0 °C and 1 °C) could maintain pear firmness and skin colour similar to those of the benchmark. Furthermore, DCA storage at -1 °C maintained the firmness even better, while no difference was observed in skin colour. However, pear fruit stored for 6 months under DCA at +1 °C were susceptible to internal

445 browning and core breakdown. Verlinden et al. (2002) reported that the core breakdown of
446 'Conference' pear is more likely to occur when fruit are stored at lower O_2, higher CO_2, and
447 higher temperature. Therefore, despite the potential energy saving of DCA storage at +1 °C,
448 this condition is not suitable for commercializing the long-term stored pear to market. In
449 contrast, DCA storage at -1 °C appears to be optimal for maintaining overall quality and saving
450 energy. This highlights the trade-off between energy savings through elevated temperature and
451 the risk of quality deterioration during long-term storage.

452 Finally, we found that the heat load produced by the fan contributed to up to 40-50 % of the
453 total heat load during storage, consistent with the findings of Ambaw et al. (2016). The
454 environmental heat load was the second largest heat load (30-40 %), while the respiration heat
455 only accounted for 10-30 % of the total heat load. Furthermore, fan load may be observed to
456 decrease with higher storage temperature and either lower O_2 level or 1-MCP treatment since
457 the total heat load into a room decreases, which can lead to shorter running time of the
458 evaporator fan system (Kittemann et al., 2015; Büchele et al., 2023a). However, in this study,
459 we assumed a constant fan power due to limited data on fan operation. Consequently, while
460 DCA storage reduces respiratory heat production, our findings imply that to achieve energy
461 efficiency in industrial fruit storage, efforts to optimize fan operation and building insulation
462 are necessary (East et al., 2013; Ambaw et al., 2016; Gruyters et al., 2018; Akerma et al., 2020).

463 # 5. Conclusion

464 This study investigated potential energy savings that could be realised during long-term storage
465 of 'Conference' pear. Different storage strategies were implemented, i.e., DCA storage at
466 different temperatures and CA storage at different temperatures and O_2 levels, and their
467 benefits were compared relative to standard CA storage (-1 °C, 3 kPa O_2). Across all
468 conditions, fan load was responsible for up to 50 % of the total heat load, while the respiratory
469 heat only contributed for approximately 10-30 %. Based on direct respiration measurements,
470 we found that DCA storage could reduce the respiratory heat by 30-40 % compared to standard
471 CA storage, even at slightly elevated temperatures. However, higher temperatures did not
472 always reduce the total heat load for the storage system because the decreased environmental
473 heat load was traded off by the increased respiratory heat. Furthermore, at higher temperatures,
474 pears were susceptible to internal browning and core breakdown after long-term storage. Our
475 findings revealed that pear fruit stored under DCA at -1 °C saved 8 % of energy and did not
476 lead to browning. These fruit also maintained firmness and skin colour better during subsequent

shelf-life than those stored under standard CA conditions. Therefore, DCA storage at -1°C appears to balance quality maintenance and energy consumption across all experimental conditions. Despite the limited number of replicates in this study, the methodology offers a practical framework to evaluate storage strategies in an industrial setting. Future research should validate these findings across different cultivars, seasons, and storage configurations to refine storage strategies with the aim of both saving energy and retaining quality.

6. Declaration of competing interest

The authors declare that they have no known competing financial interests or personal relationships that could have appeared to influence the work reported in this paper.

7. CrediT author statement

Hoang Minh Phan: Conceptualization, Methodology, Investigation, Formal Analysis, Visualization, Writing-Original Draft. **Bert E. Verlinden**: Conceptualization, Methodology, Writing - Review & Editing. **Maarten L.A.T.M. Hertog**: Writing - Review & Editing. **Pieter Verboven**: Writing - Review & Editing, Funding acquisition. **Bart M. Nicolai**: Supervision, Writing - Review & Editing, Funding acquisition.

8. Acknowledgments

This project has received funding from the European Union's Horizon 2020 research and innovation programme under grant agreement No 101036588, European food chain supply to reduce GHG emissions by 2050 (ENOUGH). The authors also acknowledge support of Flanders Innovation and Entrepreneurship (VLAIO ICON INFLEX HBC.2022.0677).

9. References

Akerma, M., Hoang, H.M., Leducq, D., Delahaye, A., 2020. Experimental characterization of demand response in a refrigerated cold room. International Journal of Refrigeration 113, 256–265. https://doi.org/10.1016/J.IJREFRIG.2020.02.006

Ambaw, A., Bessemans, N., Gruyters, W., Gwanpua, S.G., Schenk, A., De Roeck, A., Delele, M.A., Verboven, P., Nicolaï, B.M., 2016. Analysis of the spatiotemporal temperature fluctuations inside an apple cool store in response to energy use concerns. International Journal of Refrigeration 66, 156–168. https://doi.org/10.1016/j.ijrefrig.2016.02.004

Atkins, P.W., De Paula, J., 2011. Physical chemistry for the life sciences, 2nd ed. ed. W.H. Freeman and Co. : Oxford University Press, New York, Oxford.

Bessemans, N., Verboven, P., Verlinden, B.E., Nicolaï, B.M., 2016. A novel type of dynamic controlled atmosphere storage based on the respiratory quotient (RQ-DCA). Postharvest Biology and Technology 115, 91–102. https://doi.org/10.1016/j.postharvbio.2015.12.019

Boeckx, J., Pols, S., Hertog, M.L.A.T.M., Nicolaï, B.M., 2019. Regulation of the Central Carbon Metabolism in Apple Fruit Exposed to Postharvest Low-Oxygen Stress. Front. Plant Sci. 10. https://doi.org/10.3389/fpls.2019.01384

Boschiero, M., Zanotelli, D., Ciarapica, F.E., Fadanelli, L., Tagliavini, M., 2019. Greenhouse gas emissions and energy consumption during the post-harvest life of apples as affected by storage type, packaging and transport. Journal of Cleaner Production 220, 45–56. https://doi.org/10.1016/j.jclepro.2019.01.300

Büchele, F., Khera, K., Thewes, F.R., Kittemann, D., Neuwald, D.A., 2023a. Dynamic Control of Atmosphere and Temperature Based on Fruit CO2 Production: Practical Application in Apple Storage and Effects on Metabolism, Quality, and Volatile Profiles. Food Bioprocess Technol 16, 2497–2510. https://doi.org/10.1007/s11947-023-03079-0

Büchele, F., Thewes, F.R., Khera, K., Voegele, R.T., Neuwald, D.A., 2023b. Impacts of dynamic controlled atmosphere and temperature on physiological disorder incidences, fruit quality and the volatile profile of “Braeburn” apples. Scientia Horticulturae 317, 112072. https://doi.org/10.1016/j.scienta.2023.112072

Bulens, I., Van de Poel, B., Hertog, M.L.A.T.M., De Proft, M.P., Geeraerd, A.H., Nicolaï, B.M., 2011. Protocol: An updated integrated methodology for analysis of metabolites and enzyme activities of ethylene biosynthesis. Plant Methods 7. https://doi.org/10.1186/1746-4811-7-17

De Wild, H.P.J., Woltering, E.J., Peppelenbos1, H.W., 1999. Carbon dioxide and 1-MCP inhibit ethylene production and respiration of pear fruit by different mechanisms. Journal of Experimental Botany 50, 837–844. https://doi.org/10.1093/jxb/50.335.837

East, A.R., Smale, N.J., Trujillo, F.J., 2013. Potential for energy cost savings by utilising alternative temperature control strategies for controlled atmosphere stored apples. International Journal of Refrigeration 36, 1109–1117. https://doi.org/10.1016/j.ijrefrig.2012.10.028

Franck, C., Lammertyn, J., Ho, Q.T., Verboven, P., Verlinden, B., Nicolaï, B.M., 2007. Browning disorders in pear fruit. Postharvest Biology and Technology 43, 1–13. https://doi.org/10.1016/j.postharvbio.2006.08.008

Gruyters, W., Verboven, P., Delele, M., Gwanpua, S.G., Schenk, A., Nicolaï, B., 2018. A numerical evaluation of adaptive on-off cooling strategies for energy savings during long-term storage of apples. International Journal of Refrigeration 85, 431–440. https://doi.org/10.1016/j.ijrefrig.2017.10.018

Ho, Q.T., Hertog, M.L.A.T.M., Verboven, P., Ambaw, A., Rogge, S., Verlinden, B.E., Nicolaï, B.M., 2018. Down-regulation of respiration in pear fruit depends on temperature. Journal of Experimental Botany 69, 2049–2060. https://doi.org/10.1093/JXB/ERY031

Ho, Q.T., Verboven, P., Verlinden, B.E., Lammertyn, J., Vandewalle, S., Nicolaï, B.M., 2008. A continuum model for metabolic gas exchange in pear fruit. PLOS Computational Biology 4, e1000023. https://doi.org/10.1371/JOURNAL.PCBI.1000023

Ho, Q.T., Verboven, P., Verlinden, B.E., Schenk, A., Delele, M.A., Rolletschek, H., Vercammen, J., Nicolaï, B.M., 2010. Genotype effects on internal gas gradients in apple fruit. Journal of Experimental Botany 61, 2745–2755. https://doi.org/10.1093/jxb/erq108

Johnston, J.W., Hewett, E.W., Hertog, M.L.A.T.M., Harker, F.R., 2002. Temperature and ethylene affect induction of rapid softening in 'Granny Smith' and 'Pacific Rose™' apple cultivars. Postharvest Biology and Technology 25, 257–264. https://doi.org/10.1016/S0925-5214(01)00194-6

Kittemann, D., McCormick, R., Neuwald, D.A., 2015. Effect of high temperature and 1-MCP application or dynamic controlled atmosphere on energy savings during apple storage. Europ.J.Hort.Sci. 80, 33–38. https://doi.org/10.17660/eJHS.2015/80.1.5

Lammertyn, J., Franck, C., Verlinden, B.E., Nicolaï, B.M., 2001. Comparative study of the O2 , CO2 and temperature effect on respiration between "Conference" pear cell protoplasts in suspension and intact pears. Journal of Experimental Botany 52, 1769–1777. https://doi.org/10.1093/jexbot/52.362.1769

Lieberz, S., 2024. Prognosfruit 2024 - EU Production Down for Apples Up for Pears (Voluntary No. GM2024- 0008). World Apple and Pear Association, Germany.

Llopis, R., Martínez-Ángeles, M., 2026. Enhancing CO2 supermarket refrigeration efficiency by raising the medium-evaporation temperature through zero-superheat operation. International Journal of Refrigeration 181, 253–265. https://doi.org/10.1016/j.ijrefrig.2025.10.021

Nahor, H.B., Scheerlinck, N., Verboven, P., Van Impe, J., Nicolaï, B.M., 2005. A continuous/discrete simulation of controlled atmosphere (CA) cool storage systems: Evaluation of plant performance/design and product quality evolution. International Journal of Refrigeration 28, 471–480. https://doi.org/10.1016/j.ijrefrig.2004.11.010

Prange, R.K., 2018. Dynamic controlled atmosphere (DCA) storage of fruits and vegetables. Reference Module in Food Science. https://doi.org/10.1016/b978-0-08-100596-5.21349-8

Saquet, A.A., Streif, J., 2017. Respiration rate and ethylene metabolism of 'jonagold' apple and 'conference' pear under regular air and controlled atmosphere. Bragantia 76, 335–344. https://doi.org/10.1590/1678-4499.189

Seabold, S., Perktold, J., 2010. Statsmodels: Econometric and Statistical Modeling with Python. scipy. https://doi.org/10.25080/Majora-92bf1922-011

Thewes, Fabio Rodrigo, Brackmann, A., Both, V., Anese, R.D.O., Schultz, E.E., Ludwig, V., Wendt, L.M., Berghetti, M.R.P., Thewes, Flavio Roberto, 2020. Dynamic controlled atmosphere based on carbon dioxide production (DCA – CD): Lower oxygen limit establishment, metabolism and overall quality of apples after long-term storage. Postharvest Biology and Technology 168, 111285. https://doi.org/10.1016/j.postharvbio.2020.111285

Thewes, F.R., Both, V., Brackmann, A., Weber, A., de Oliveira Anese, R., 2015. Dynamic controlled atmosphere and ultralow oxygen storage on 'Gala' mutants quality maintenance. Food Chemistry 188, 62–70. https://doi.org/10.1016/j.foodchem.2015.04.128

Vallat, R., 2018. Pingouin: statistics in Python. Journal of Open Source Software 3, 1026. https://doi.org/10.21105/joss.01026

Verlinden, B.E., Bessemans, N., Verboven, P., Nicolaï, B.M., 2023. Saving energy using RQ-based dynamic controlled atmosphere storage of blueberry fruit., in: Proceedings of the 26th IIR International Congress of Refrigeration: Paris , France, August 21-25, 2023. https://doi.org/10.18462/iir.icr.2023.0954

Verlinden, B.E., de Jager, A., Lammertyn, J., Schotsmans, W., Nicolaï, B.M., 2002. Effect of Harvest and delaying Controlled Atmosphere Storage Conditions on Core Breakdown Incidence in 'Conference' Pears. Biosystems Engineering 83, 339–347. https://doi.org/10.1006/bioe.2002.0127

Virtanen, P., Gommers, R., Oliphant, T.E., Haberland, M., Reddy, T., Cournapeau, D., Burovski, E., Peterson, P., Weckesser, W., Bright, J., Van Der Walt, S.J., Brett, M., Wilson, J., Millman, K.J., Mayorov, N., Nelson, A.R.J., Jones, E., Kern, R., Larson, E., Carey, C.J., Polat, İ., Feng, Y., Moore, E.W., VanderPlas, J., Laxalde, D., Perktold, J., Cimrman, R., Henriksen, I., Quintero, E.A., Harris, C.R., Archibald, A.M., Ribeiro, A.H., Pedregosa, F., Van Mulbregt, P., SciPy 1.0 Contributors, Vijaykumar, A., Bardelli, A.P., Rothberg, A., Hilboll, A., Kloeckner, A., Scopatz, A., Lee, A., Rokem, A., Woods, C.N., Fulton, C., Masson, C., Häggström, C., Fitzgerald, C., Nicholson, D.A., Hagen, D.R., Pasechnik, D.V., Olivetti, E., Martin, E., Wieser, E., Silva, F., Lenders, F., Wilhelm, F., Young, G., Price, G.A., Ingold, G.-L., Allen, G.E., Lee, G.R., Audren, H., Probst, I., Dietrich, J.P., Silterra, J., Webber, J.T., Slavič, J., Nothman, J., Buchner, J., Kulick, J., Schönberger, J.L., De Miranda Cardoso, J.V., Reimer, J., Harrington, J., Rodríguez, J.L.C., Nunez-Iglesias, J., Kuczynski, J., Tritz, K., Thoma, M., Newville, M., Kümmerer, M., Bolingbroke, M., Tartre, M., Pak, M., Smith, N.J., Nowaczyk, N., Shebanov, N., Pavlyk, O., Brodtkorb, P.A., Lee, P., McGibbon, R.T., Feldbauer, R., Lewis, S., Tygier, S., Sievert, S., Vigna, S., Peterson, S., More, S., Pudlik, T., Oshima, T., Pingel, T.J., Robitaille, T.P., Spura, T., Jones, T.R., Cera, T., Leslie, T., Zito, T., Krauss, T., Upadhyay, U., Halchenko, Y.O., Vázquez-Baeza, Y., 2020. SciPy 1.0: fundamental algorithms for scientific computing in Python. Nat Methods 17, 261–272. https://doi.org/10.1038/s41592-019-0686-2

Weber, A., Thewes, F.R., Anese, R.D.O., Both, V., Pavanello, E.P., Brackmann, A., 2017. Dynamic controlled atmosphere (DCA): interaction between DCA methods and 1-methylcyclopropene on 'Fuji Suprema' apple quality. Food Chemistry 235, 136–144. https://doi.org/10.1016/j.foodchem.2017.05.047

Wendt, L.M., Ludwig, V., Thewes, Fabio Rodrigo, Soldateli, F.J., Batista, C.B., Thewes, Flavio Roberto, Fukui, C.M., Brackmann, A., Both, V., Katsurayama, J.M., 2024a.

633 Dynamic controlled atmosphere monitored by respiratory quotient as a new method to
634 store pears: Effect on the volatile compounds profile and general quality. Postharvest
635 Biology and Technology 209, 112721.
636 https://doi.org/10.1016/j.postharvbio.2023.112721
637 Wendt, L.M., Ludwig, V., Thewes, F.R., Soldateli, F.J., Batista, C.B., Fukui, C.M.,
638 Gonçalves Dos Santos, G., Katsurayama, J.M., Brackmann, A., Both, V., 2024b.
639 Effect of dynamic controlled atmosphere on volatile compound profile and quality of
640 pears. Scientia Horticulturae 328, 112910.
641 https://doi.org/10.1016/j.scienta.2024.112910
642